SCIENTIFIC REPORTS

OPEN

SUBJECT AREAS:
THERMODYNAMICS
PROTEIN FOLDING
BIOPHYSICAL CHEMISTRY
FLUORESCENCE SPECTROMETRY

Received
25 June 2014

Accepted
15 September 2014

Published
30 September 2014

Correspondence and requests for materials should be addressed to R.M. (maha@iiserb.ac.in.)

* These authors contributed equally to this work.

Differential Contribution of Tryptophans to the Folding and Stability of the Attachment Invasion Locus Transmembrane β-Barrel from *Yersinia pestis*

Ankit Gupta*, Punit Zadafiya* & Radhakrishnan Mahalakshmi

Molecular Biophysics Laboratory, Department of Biological Sciences, Indian Institute of Science Education and Research, Bhopal. India.

Attachment invasion locus (Ail) protein of *Yersinia pestis* is a crucial outer membrane protein for host invasion and determines bacterial survival within the host. Despite its importance in pathogenicity, surprisingly little is known on Ail biophysical properties. We investigate the contribution of micelle concentrations and interface tryptophans on the Ail β-barrel refolding and unfolding processes. Our results reveal that barrel folding is surprisingly independent of micelle amounts, but proceeds through an on-pathway intermediate that requires the interface W42 for cooperative barrel refolding. On the contrary, the unfolding event is strongly controlled by absolute micelle concentrations. We find that upon Trp→Phe substitution, protein stabilities follow the order W149F>WT>W42F for the refolding, and W42F>WT>W149F for unfolding. W42 confers cooperativity in barrel folding, and W149 clamps the post-folded barrel structure to its micelle environment. Our analyses reveal, for the first time, that interface tryptophan mutation can indeed render greater β-barrel stability. Furthermore, hysteresis in Ail stems from differential barrel-detergent interaction strengths in a micelle concentration-dependent manner, largely mediated by W149. The kinetically stabilized Ail β-barrel has strategically positioned tryptophans to balance efficient refolding and subsequent β-barrel stability, and may be evolutionarily chosen for optimal functioning of Ail during *Yersinia* pathogenesis.

Transmembrane (TM) proteins are, by and large, 'kinetically trapped' in biological systems[1–4]. Early evidences that Anfinsen's equilibrium thermodynamic model for refolding soluble proteins cannot be extended to membrane proteins arose in the '90s, from studies of multi-pass hydrophobic helices by Popot, Engelman and others[5–12]. The folding process of TM helices fit well to a two-stage model which described each helix as an autonomous folding unit that assembled in the apolar interior of the lipid bilayer by an intricate, largely irreversible, mechanism following alternative pathways for protein assembly (folding) and dissociation (unfolding)[3,5,8,13]. TM β-barrels are also known to adopt a multi-step refolding event which oftentimes involves rapid protein collapse and adsorption onto the lipid bilayer, followed by a much slower insertion event that culminates in barrel assembly[1,12,14,15].

Speculation on whether Anfinsen's hypothesis would be extendable to membrane proteins, owing to their unique membrane environment, was resolved when more recent studies demonstrated that *in vitro* refolded TM β-barrels of bacterial and human origin are in thermodynamic equilibrium[12,14–18]. Such systems follow superimposable reversible pathways for refolding and unfolding *in vitro*, in the carefully screened lipid and buffer conditions that permit such equilibrium[10,15,19]. The native protein conformation in such cases is a consequence of the Gibbs free energy minimum achieved by the system, and the folding event itself is entropically driven and enthalpically balanced. Not surprisingly, however, as Popot and Engelman surmised[5,8], most membrane proteins do not exist in thermodynamic equilibrium, and are plagued by hysteresis[2,4,10–12,20]. A 'hysteresis loop', or 'open loop', is a condition wherein microscopic differences in a system's configuration perturb thermodynamic equilibrium, sacrificing the free energy minimum for a presumably enhanced functionality[11].

In a large population of TM proteins, the kinetics of interconversion between the folded state and unfolded form, through metastable intermediates, gives rise to hysteresis in an otherwise equilibrium system[4,10–12]. Such systems are trapped by kinetic stabilization, a process that is influenced by residue-specific protein-protein and protein-lipid interactions, lipid or detergent morphology and the inherent tendency of hydrophobic proteins to form stable aggregates outside their lipid environment. Hence, despite the reversibility observed in a handful of TM β-barrels thus far, the more pressing question is the cause of hysteresis in these proteins. The wide repertoire of refolding methodologies and membrane mimetics used for the 8–24 stranded TM β-barrels *in vitro*[21], as well as the influence of parameters such as temperature and pH, employed in the reaction, on the physical properties of the lipid or detergent[10–12,22], point towards diversity in the metastable states populating the folding and unfolding pathways. Identification of key elements in the protein which contribute to hysteresis, would allow us to understand β-barrel refolding *in vitro* and shed light on membrane protein recycling *in vivo*.

We probed the factors contributing to the kinetic component of membrane protein stability using the 17.6 kDa 8-stranded TM β-barrel Ail from *Yersinia pestis*, the causative agent of bubonic, pneumonic and septicemic plague, as our model system. The **A**ttachment **i**nvasion **l**ocus (Ail) protein belongs to the Ail/Lom family of outer membrane proteins coded by the y1324 locus in both KIM and CO92 strains of *Y. pestis*, and is present only in pathogenic *Yersiniae*[23,24]. Ail expression levels coincide with the pathogenicity of the host bacterium, owing to its associated role in virulence[25,26], and it functions in adhesion and internalization of the bacterium into host cells through Yop delivery and 'attack complex' formation *in vivo*[25,27,28]. Ail also confers serum resistance to complement-mediated bacteriolysis, blocking phagocytosis and survival within macrophages[26–28], and is therefore one of the prime targets for drug development against this category A bioterrorism agent.

Demarcation of the transmembrane and loop regions of Ail, and other TM β-barrel is achieved by the aryl groups populating the 'aromatic girdles', which defines barrel depth and the lipid or micelle interaction interface[29–36]. Aryl residues mediate structural stability and associated 'invasin' property of Ail[23], exposing binding pockets for protein function. Stereospecifically positioned aromatics therefore play a key role in barrel formation (folding), stability (susceptibility to unfolding), depth definition (TM span) and activity[29,31–33,35–39]. Biophysical characterization of how Ail interacts with its folding environment, and the contribution of aromatics, particularly Trp residues, would therefore throw light on protein behaviour.

Herein, we address the impact of micelle-protein interaction and the aryl moiety tryptophan, on the thermodynamic *versus* kinetic stability of Ail. We demonstrate that, of the two indoles, the Trp required for Ail refolding in lauryldimethylamine oxide (LDAO) micelles is different from the Trp that confers subsequent barrel stability. Furthermore, DPR (detergent-to-protein ratio) holds significant bearing on protein unfolding, while the effect on the refolding event is less significant. Such differential contribution of Trp residues has not been observed thus far for other known 8-stranded TM β-barrels. We discuss the implications of hysteresis, and the associated contribution of aryl groups, on Ail function and barrel stability in *Yersiniae*.

Results

Tryptophans reside in unique local environments but do not affect Ail refolding ability. *Yersinia* Ail possesses two Trp residues[25]; the crystal structure maps W42 to the membrane interface whereas W149 is slightly closer to the lipid core (Fig. 1a). To assess the influence of Trp mutations on β-barrel formation, we carried out gel mobility shift assays[24,40–42], of unboiled Ail samples refolded in 20 mM, 50 mM and 100 mM LDAO. Wild type Ail (Ail-WT) and the single Trp mutants (Ail-W42F and Ail-W149F) exhibit retarded gel mobility, and migrate at ~24 kDa on SDS-PAGE (Fig. 1b), indicating protein folding and barrel formation in the three DPRs used in this study. Ail, thus refolded, retains the ability to bind heparin[25] (not shown), and exhibits resistance to proteolysis by proteinase K (Fig. 1b), suggesting that a Trp→Phe substitution does not affect the ability of Ail to refold in various LDAO concentrations. Comparable secondary structure content for all three proteins from circular dichroism measurements (not shown), substantiates this observation.

Interestingly, Ail exhibits oligomeric forms on SDS-PAGE gels of unboiled samples (Fig. 1b). Ail multimerization has not been observed earlier, and no known function has been associated with Ail multimers. It is therefore likely that the higher order oligomers are an artefact of *in vitro* conditions. In high DPR, the oligomeric forms are lowered, supporting a non-specific barrel association that may be diffusion driven. A similar behaviour has been observed earlier for OmpA[43] and OmpX[44], both 8-stranded barrels structurally similar to Ail. Notably, oligomerization is highest in W149F, which may perhaps bear implications on barrel behaviour.

Using acrylamide quenching measurements, we examined the accessibility of the indole ring, to probe for possible variations in the local Trp environment of the three proteins. Our data (Fig. 1c) indicates that W42 (W149F mutant) undergoes an increase in indole solvent accessibility with increasing LDAO (and DPR), reflected in the increase in the K_{SV} value. This may arise from contributions from static and dynamic quenching of W42 fluorescence by acrylamide or complex protein-micelle-quencher interactions (see Supplementary Fig. 1).W42F and WT constructs show lower K_{SV} values that do not change significantly with LDAO concentration (Fig. 1c), suggesting that tryptophans in these proteins are occluded from acrylamide.

A better insight to the Trp environment can be obtained from measurements of average lifetime ($<\tau>$) and calculation of the bimolecular quenching constant (k_q) (Table 1). The former provides information on the rigidity (longer lifetimes indicate the presence of a rigid fluorophore), while the latter specifies the degree of solvent exposure of the fluorophore[45]. Interestingly, W149 (W42F mutant) shows the lowest lifetime, despite being buried. In contrast, W42 (W149F mutant) displays higher lifetimes that show a strong DPR dependence, coupled with higher Trp anisotropy. This together indicates that the W149 side chain is conformationally mobile, despite residing in a micellar environment (low K_{SV}). W42, however, becomes increasingly immobile in high DPR, due to its location at the interface, thereby displaying higher lifetime and anisotropy, as a consequence of poor non-radiative losses in fluorescence. The WT displays an intermediate behaviour with values closer to W42F, possibly balancing favourable solvent-indole interactions for both W42 and W149.

Reported k_q values for moderately exposed Trp residues are typically $<1.5 \times 10^9$ $M^{-1}s^{-1}$, while solvent (and thereby quencher) accessible indoles display $k_q > 1.5 \times 10^9$ $M^{-1}s^{-1}$ [45,46]. In low DPRs, W149F particularly possesses the most solvent-accessible Trp ($k_q = 1.85 \times 10^9$ $M^{-1}s^{-1}$; Table 1), while in high DPRs, the k_q is lowered in all three proteins, with WT and W42F now possessing relatively less exposed Trp residues compared to W149F. However, since all the k_q values are within the accepted range for moderately exposed indoles (k_q for buried Trp lies in the $0.6–1.0 \times 10^9$ $M^{-1}s^{-1}$ range[45,46]), we propose that all three proteins show the presence of interfacial Trp residue(s); differences arising from their respective interaction pockets give rise to the observed variation in K_{SV} and $<\tau>$. Put together, these properties provide the order WT ≥ W42F > W149F for increase in solvent exposure of the indole. Both Trp residues in Ail therefore reside in different local environments and possess features that are uniquely modulated by their surroundings; however, this does not influence barrel refolding.

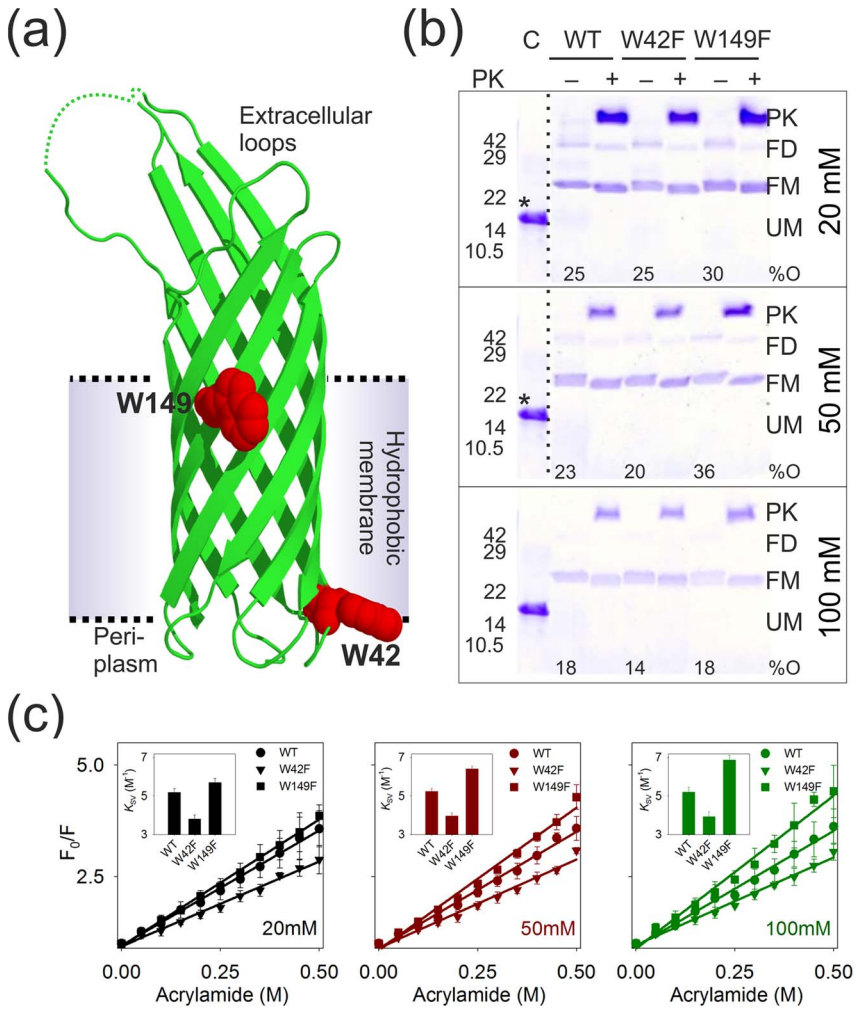

Figure 1 | Response of Trp residues of Ail to DPR and its influence on Ail refolding. (a) Ribbon diagram of Ail obtained from the crystal structure (PDBID: 3QRA[25]) highlighting the two Trp residues as red spheres. The putative transmembrane segment is also indicated. Segments of two extracellular loops, absent in the structure, are denoted as dotted lines. (b) SDS-PAGE gel mobility shift assay of unboiled Ail-WT, W42F and W149F samples refolded in 20 mM (top), 50 mM (middle) and 100 mM (bottom) LDAO. Refolded samples also subjected to pulse proteolysis using proteinase K (PK) are indicated as (+) and undigested samples as (-). Bands corresponding to the folded dimer (FD) and higher order oligomers are most prominent in the 20 mM LDAO sample. Refolded monomer (FM), migrating at ~24 kDa, and the unfolded monomer (UM) migrating at ~17.0 kDa, are also marked. Unfolded Ail in 8.0 M urea served as the control (C). The percentage of observed Ail oligomers (%O) in each condition was quantified by densitometry[42], and is provided below the respective sample lanes. Band positions of molecular weight standards are indicated beside each gel. The unfolded control from the bottom gel has been shown in the top and middle gels, and is marked (*). Dotted lines separate different sections of gels that have been presented together. Note that the various DPRs underwent different dilutions before SDS-PAGE (to minimize interference from LDAO on band migration), and therefore protein concentrations across the three gels are not similar. (c) Plot of Trp fluorescence quenching of Ail-WT (circles), W42F (inverted triangles) and W149F (squares) with increasing acrylamide concentrations, fitted to a linear equation (fits are shown as lines), to obtain the Stern-Volmer constant (K_{SV}) (shown as inset). Shown here are data obtained in 20 mM (black), 50 mM (red) and 100 mM (green) LDAO. Note that the W149F construct displays an increase in K_{SV} upon addition of LDAO, whereas corresponding values for the WT and W42F proteins are largely DPR insensitive (also see Supplementary Fig. 1). K_{SV} values for unfolded Ail (in 8.0 M GdnHCl; all three constructs) was ~7.4 M^{-1} and aggregated Ail was ~3.1 M^{-1}.

Ail refolding is largely DPR independent but displays an LDAO-stabilized intermediate. Dilution of guanidine hydrochloride (GdnHCl)-denatured Ail drives rapid barrel formation within minutes, in LDAO. We therefore monitored the refolding process of Ail-WT, W42F and W149F using a GdnHCl gradient and Trp fluorescence as the probe. A typical emission profile acquired at 48 h is shown in Fig. 2a. The C_m values (chemical denaturation mid-point) derived from folded fractions (f_F) calculated at the $\lambda_{em\text{-}max}$ for the folded protein (330 nm) or the observed anisotropy values (Fig. 2b and Supplementary Figs. 2–4), are provided in Fig. 2c. In 50 mM and 100 mM LDAO, the anisotropy C_m shows lowering and f_F C_m increases in all three proteins; the global change in C_m is, however, marginal. We observe considerable differences in the C_m values derived from Trp fluorescence and anisotropy measurements between the various proteins only in low DPRs. Furthermore, in 20 mM LDAO, WT shows a high anisotropy C_m that could arise from association of unfolded Ail with LDAO moieties at the vicinity of both Trp residues, thereby nucleating refolding. The W42F mutant, which lacks the interface Trp residue, has the lowest C_m, and requires sufficient lowering of GdnHCl for refolding.

Marginal differences in the C_m (f_F) and C_m (anisotropy) suggest that barrel refolding conceivably proceeds by sequestering LDAO in micelle-binding hydrophobic pockets, following which the barrel assembles only at the threshold GdnHCl concentration, in a DPR-independent manner. Interestingly, we noticed the population of a possible folding intermediate in high DPR, which appeared in the

Table 1 | Summary of Trp fluorescence parameters measured for Ail-WT and its Trp mutants in various DPRs

	Average lifetime (<τ>, ns)[b]			Anisotropy (r)[b]			Bimolecular quenching constant (k_q, × 10^9 M^{-1} s^{-1})		
DPR[a]	WT	W42F	W149F	WT	W42F	W149F	WT	W42F	W149F
700 : 1	3.62 ± 0.2	2.43 ± 0.2	3.17 ± 0.1	0.143	0.122	0.152	1.40	1.54	1.85
700 : 1 (D)	1.96 ± 0.0	1.68 ± 0.1	1.77 ± 0.1	0.068	0.070	0.062	-	-	-
1750 : 1	3.96 ± 0.1	2.93 ± 0.2	3.72 ± 0.3	0.140	0.123	0.159	1.33	1.36	1.77
1750 : 1(D)	2.10 ± 0.1	1.75 ± 0.1	1.87 ± 0.1	0.080	0.068	0.072	-	-	-
3500 : 1	3.97 ± 0.1	2.89 ± 0.1	4.34 ± 0.1	0.141	0.120	0.154	1.31	1.35	1.56
3500 : 1 (D)	2.18 ± 0.1	1.81 ± 0.0	1.86 ± 0.0	0.106	0.080	0.069	-	-	-
0:1 (U)	1.75 ± 0.1	1.66 ± 0.1	1.61 ± 0.1	0.050	0.046	0.047	4.18	4.31	4.78
0:1 (A)	0.32 ± 0.0[c]	0.14 ± 0.0[c]	0.20 ± 0.0[c]	0.123	0.143	0.142	-[c]	-[c]	-[c]

[a]Here (D) represents the refolded protein denatured by the addition of 6.4 M GdnHCl, and therefore retains the respective LDAO amounts. (U) is unfolded protein in 8.0 M GdnHCl and contains no LDAO. (A) is aggregated protein sample prepared in Tris-HCl pH 8.5 and contains 0.16 M GdnHCl.
[b]All samples were incubated for 48 h at 25°C before obtaining measurements. $<\tau> = \Sigma\tau = \alpha_i\tau_i$
[c]Lifetimes could not be accurately determined due to interference from scattering. Hence, the k_q values were also not calculated.

order W42F > WT > W149F (arrow in Fig. 2b f_F plots). To probe this further, we examined Ail refolding in 200 mM LDAO (DPR 7000 : 1) (Fig. 3a). The data not only clearly demonstrates the presence of a refolding intermediate in all three Ail constructs (three-state unfolding) but also its surprising absence in the corresponding anisotropy measurements (two-state transition). The C_m for the transition from intermediate to folded protein obtained from f_F data compares well with the anisotropy C_m (Fig. 3b), suggesting that W42 and/or W149 in the folding intermediate experiences a change in the polarity of its local environment but retains side chain mobility. Such behaviour mimics the transition of the amphipathic indole from a polar (solvent-exposed) to apolar (lipid- or micelle-exposed) environment before completion of the folding process, and is characteristic of a vesicle-adsorbed barrel intermediate[1]. In our micellar systems, aromatic residues at the two girdles could sequester LDAO to nucleate barrel formation, which we observe as a blue-shifted $\lambda_{em\text{-}max}$ for the mobile fluorophore.

Surprisingly, a uniform lowering of the C_m is observed in all three proteins in high DPR (7000 : 1; compare Fig. 2c and Fig. 3b), with the values now bearing semblance to the data from 20 mM LDAO, suggesting that the stability of folded Ail is marginally lowered. Barrel stability therefore exhibits a non-linear dependence on micelle concentrations. Tight micelle packing in 200 mM LDAO is less tolerant to perturbations of the micellar forms by the protein, thereby lowering the folding efficiency of Ail, and promoting the formation of a stabilized (adsorbed) intermediate. Such acute DPR dependence has been observed previously for the human VDAC-2 19-stranded barrel[20], and may be a property of the LDAO micelles. This effect is most dramatic in Ail-W42F, which also shows lower unfolding cooperativity (m_{app} values in Supplementary Table 1), with changes in DPR. The conspicuous DPR dependence of this mutant indicates that W42 plays a crucial role in driving proper refolding of Ail.

The $\Delta G^{0,F}_{app}$ and m_{app} values calculated for the refolding process are summarized in Supplementary Table 1 (also see Supplementary Fig. 4). As the C_m values are largely similar up to 100 mM LDAO, marginal variations in the $\Delta G^{0,F}_{app}$ therefore arise from changes in the cooperativity of the refolding process. This is affected both by the LDAO concentration as well as the Trp mutation. The $\Delta G^{0,F}_{app}$ values are low in 20 mM LDAO, as anticipated. With increase in LDAO, $\Delta G^{0,F}_{app}$ increases due to an increase in the refolding cooperativity (Supplementary Fig. 4). Very high LDAO (200 mM), however, lowers these thermodynamic parameters for all three proteins. Furthermore, in Ail-W42F, the barrel folding cooperativity is lowered, thereby affecting the m_{app}, and accounts for the lowest $\Delta G^{0,F}_{app}$ for this protein (Supplementary Fig. 4). Overall, our refolding experiments therefore provide us with the order W149F > WT > W42F, for cooperativity in Ail barrel formation when the denaturant concentration is lowered, in all the three DPRs. Based on our results, it also seems likely that W42 assists the barrel in overcoming the kinetic barrier stabilizing a trapped folding intermediate.

W149 determines stability of refolded Ail in a DPR-dependent manner. In GdnHCl, although (un)folding can be achieved in various LDAO concentrations, the equilibrium unfolding experiments demonstrate hysteresis within experimental time frames, which is not uncommon for TM β-barrels[10,11,15], and suggests the existence of alternate folding and unfolding pathways and/or dissimilar activation energy values in the two processes. Using Trp fluorescence (Fig. 4a and Supplementary Figs. 5–9) and anisotropy (Fig. 4c), we evaluated the contribution of tryptophan and DPR to the stability of refolded Ail, and derived the *apparent* thermodynamic parameters (Supplementary Table 1). Contrary to folding, Ail unfolding follows a two-state transition, and we do not detect intermediates in this event. Ail refolding does not depend substantially on the LDAO amounts used in the reaction. However, unfolding of all three proteins is strongly modulated by the DPR, and the presence of higher LDAO amounts delays the onset of the unfolding event (Fig. 4b). This is reflected in an increase in the C_m with increasing LDAO concentrations (Fig. 4c). Unfolding, is however, nearly completed at the highest GdnHCl concentrations (Supplementary Figs. 5–8), even with sufficient micellar forms in solution (Supplementary Figs. 10–12).

A remarkable difference between WT Ail and the single-Trp barrels is observed in the unfolding experiments. The *apparent* thermodynamic parameters derived for the *refolding* process provided us with the order W149F > WT > W42F. C_m values obtained from f_U calculations of the *unfolding* process (Fig. 4c and Supplementary Figs. 8–9), provides us with the order W42F ≥ WT > W149F, which is the exact reverse of the Ail refolding process. Furthermore, resistance of Ail to denaturation by GdnHCl increases proportionately with the LDAO concentration. Indeed, in 100 mM LDAO, WT and W42F barrels undergo complete unfolding only in the highest GdnHCl concentrations (~6.4 M) used in the experiment. This is in contrast to the lowering of the $\Delta G^{0,F}_{app}$ (folding free energy) observed for Ail in the refolding reaction in very high LDAO concentrations (Supplementary Fig. 4). Hence, our experiments suggest that Ail responds differently in the refolding and unfolding processes, when the DPR is varied (the source of hysteresis; described later).

Calculated $\Delta G^{0,U}_{app}$ values (unfolding free energy), derived from the unfolding curves are significantly lower than the $\Delta G^{0,F}_{app}$ calculated for the refolding process (Supplementary Table 1). This arises from the lower m_{app} values for the unfolding process. Further the $\Delta G^{0,U}_{app}$ only shows a marginal increase for all three proteins, with increase in DPR. Hence, despite the high C_m, we speculate that this lower

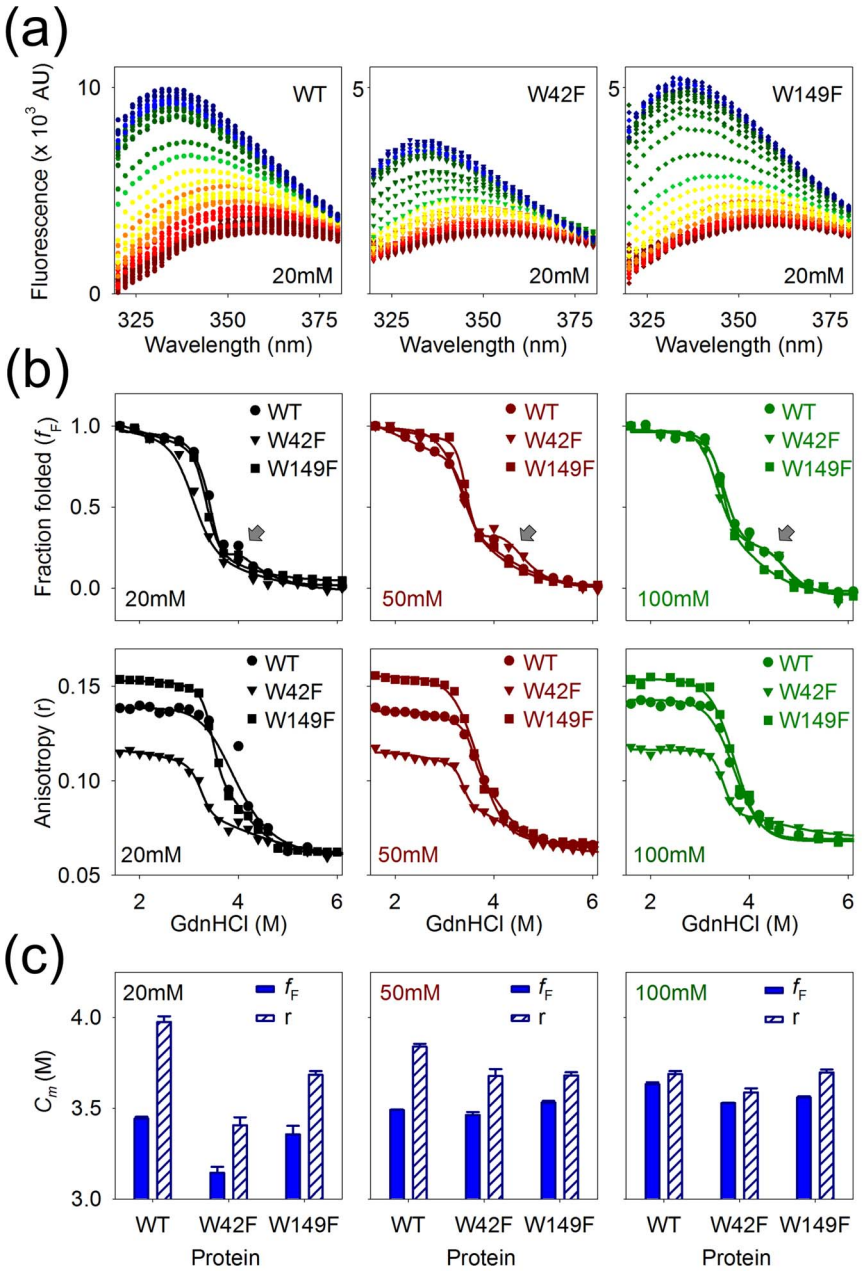

Figure 2 | Refolding of Ail in LDAO micelles is largely DPR independent. (a) Representative Trp emission profiles of Ail-WT and Trp mutants in 20 mM LDAO, highlighting the observed increase in fluorescence intensity and prominent blue shift in the $\lambda_{em\text{-}max}$ (depicted in red to blue color scheme), as the protein refolds when GdnHCl is lowered from 8.0 M to 1.6 M (red to blue). The fluorescence intensity of Trp 149 in the W42F mutant is lower than Trp 42 in the W149F mutant. This is likely to arise from non-radiative losses in Trp 149 fluorescence, although the presence of a proximal quencher cannot be eliminated. (b) Fraction folded (f_F) derived from Trp emission intensity at 330 nm (top) and corresponding anisotropy (r) values (bottom) for WT (○), W42F (▽) and W149F (□) in 20 mM (black), 50 mM (red) and 100 mM (green) LDAO. Data were collected at every 0.1 M increment of GdnHCl and the mean of two – three experiments were calculated. However, representative mean data points are shown in f_F plots without error bars, for clarity. All samples (lower GdnHCl concentrations) were checked using gel mobility shift on SDS-PAGE for completion of the refolding process. While ~100% refolding was observed, the presence of trace amounts of unfolded protein cannot be completely excluded. Representative data are shown for the anisotropy experiments. Fits are shown as solid lines and corresponding LDAO concentrations are indicated in each plot. Note the appearance of an intermediate (indicated by an arrow) at ~4.0 M GdnHCl only in the f_F plots of W42F in all LDAO concentrations, and additionally in WT in 100 mM LDAO. (c) C_m values obtained from f_F (blue, solid fill) and anisotropy (r) (blue, diagonal stripes) data are compared for the three Ail constructs across various LDAO concentrations. Note that the C_m values are different only in 20 mM LDAO (DPR 700 : 1) and are largely analogous in 50 mM (DPR 1750 : 1) and 100 mM (DPR 3500 : 1) LDAO. Error bars represent goodness of fits. Also see Supplementary Figs. 2–4.

$\Delta G^{0,U}_{app}$ arises from incomplete dissociation of LDAO from the protein, even after barrel unfolding. This causes the unfolding to be less a cooperative process, unlike the highly cooperative refolding event.

Most interestingly, the anisotropy C_m values not only follow the order WT > W42F > W149F but also escalate significantly with change in LDAO (and DPR) amounts. Despite the Trp fluorescence measurements (Fig. 4b, top panel), and SDS-PAGE analysis (not shown) indicating near-complete barrel unfolding even in the presence of intact LDAO micelles (see Supplementary Figs. 10–12), higher anisotropy values under similar conditions suggest a prepon-

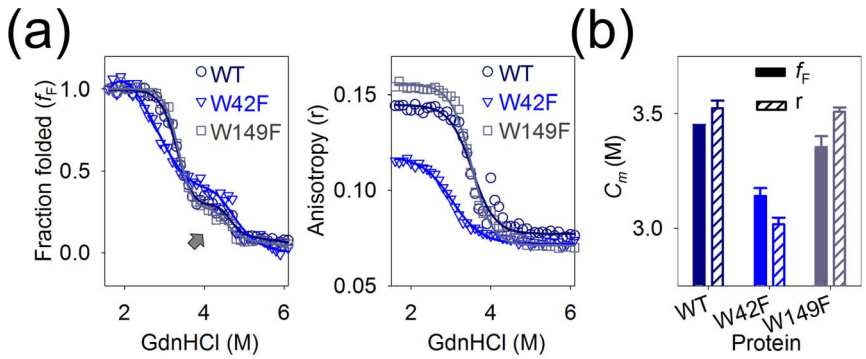

Figure 3 | A refolding intermediate of Ail is observed in high DPR. (a) Comparison of the folded fraction (f_F) and anisotropy values of Ail-WT (○, purple) and the Trp mutants W42F (▽, blue) and W149F (□, grey) refolded in 200 mM LDAO (DPR 7000 : 1) indicates the presence of a stable intermediate species in the f_F (indicated by an arrow), which is absent in the anisotropy (r) data. Fits are indicated by solid lines that are color-coded to match the corresponding symbols. (b) Plot of the C_m values calculated from the f_F (solid fill) and anisotropy (r) (diagonal stripes) data using linear extrapolation. Color codes are matched to Fig. 3a. For the f_F data, C_m reflects the mid-point of the transition of the 'adsorbed' protein intermediate to the fully refolded β-barrel form. The lowest C_m is seen in the case of W42F, suggesting destabilization of this protein in very high DPR. Also see Supplementary Figs. 2–4.

derance of LDAO-bound protein. While the anisotropy C_m is lowered with increase in LDAO for the refolding process (see Fig. 2c), we observe that the unfolding profiles show higher anisotropy with increasing LDAO. Efficient sequestering of tightly-bound LDAO, even after barrel unfolding, likely results in a complex protein-LDAO association event, leading to the higher anisotropy C_m. Such tightly bound complexes in unfolded membrane proteins have been proposed earlier[47]. Moreover, this increase is predominant in Ail-WT and Ail-W42F, pointing to a critical role of W149 in anchoring the refolded protein to its micellar environment.

Discussion

Several studies, which address the contribution of aromatic residues to the stability of β-barrel membrane proteins prefer model systems including OmpA, PagP, FomA and, to some extent, VDAC[1,14,15,18,19,32,33,36,38,40,48–51]. Mutational analyses in OmpA and PagP have attempted the Trp→Ala as well as Trp→Phe substitutions[32,33,38]; such studies have shown that the more dramatic replacement of aryl groups with aliphatic side chains in the water-bilayer interface considerably lowers the free energy of the refolded barrel. Surprisingly, however, even conserved Trp→Phe substitutions that retain the aromatic character at the mutation site, have indicated an average loss in free energy of between 1.0–2.0 kcal/mol[33]. To our knowledge, none of the studies so far have examined the role of aromatic residues in the refolding process itself. Here, we specifically addressed the requirement of the two Trp residues of *Y. pestis* Ail, on barrel folding and stability, and by selective Trp→Phe mutations, we have been able to deduce the contribution of the amphipathic Trp residue to the protein scaffold.

Cumulative analysis of the apparent thermodynamic parameters derived for the three proteins from GdnHCl-mediated (un/re)folding experiments, in the three DPRs examined (700 : 1, 20 mM LDAO; 1750 : 1, 50 mM LDAO; 3500 : 1, 100 mM LDAO) provides us with an overall variance in the order $20 < 50 \approx 100 > 200$ (mM) LDAO. The difference between C_m values derived from fits to the f_F data and anisotropy measurements are most prominent in low DPRs (Fig. 2c), suggesting that unfolded Ail has the ability to sequester LDAO molecules even prior to the barrel collapse event. This process occurs in the tryptophan vicinity, leading to the higher anisotropy C_m, and may either be independent of barrel formation or may serve as a nucleating factor for refolding. Furthermore, in the W42F mutant, accumulation of an intermediate in the refolding reaction, and based on the low m_{app} values, we propose that W42 facilitates the Ail barrel to better overcome trapped refolding intermediates, mediating a cooperative refolding process in various LDAO concentrations (Fig. 5; also see Supplementary Fig. 13). Additionally, we find that Ail refolding requires pre-formed micelles, as observed for OmpA[48], but detergent adsorption seems to precede barrel formation.

The low C_m of W42F in the refolding experiments in 20 mM LDAO merits comment (see Fig. 2c and Supplementary Fig. 13 and Supplementary Table 1). Hydrophobic interactions mediated by the 'aromatic girdle' of TM β-barrels act as critical determinants between favourable protein-lipid/detergent interactions that result in protein folding, and unfavourable protein-protein interactions that cause aggregation. Indeed, Trp residues in the aromatic girdle act as 'stop transfer' signals during the coupled membrane protein synthesis – folding process[30,52], define the 'span' of the TM region of β-barrels[52], explaining their occurrence at the bilayer interface in several membrane proteins (Table 2). Our results contradict the anticipated destabilization of W149F mutant, which lacks the transmembrane Trp. We speculate that in Ail, it is W42 (and not W149), which defines the 'barrel edge'; replacement with the more hydrophobic Phe results in pronounced stabilization of a partly folded intermediate and induces 'roughness' in the folding energy landscape of the W42F mutant, allowing trapped on-pathway intermediates to be experimentally detected (Fig. 6).

The Ail unfolding process shows a distinct variance of $20 < 50 < 100$ (mM) LDAO with a DPR- and LDAO-dependent increment of the C_m. This results in a marginal increase in the unfolding free energy; however, the cooperativity of the unfolding process is not affected (Supplementary Fig. 9). It is noteworthy that while the $\Delta G^{0,F}_{app}$ is in the approximate range of -6.0 to -11.0 kcal/mol, the $\Delta G^{0,U}_{app}$ values are significantly lowered (~4.0 kcal/mol) and have correspondingly low m_{app} values (< -1.0 kcal/mol.M). Despite the higher C_m values, the obvious loss in unfolding cooperativity (compared to the refolding cooperativity; see Fig. 5. Also see Supplementary Fig. 4 and Supplementary Fig. 9) suggests that LDAO does not stabilize Ail to the extent observed for OmpX[42] or VDAC[18]. The highest stability is observed in the W42F mutant, which retains W149, suggesting that W149 anchors the protein to the micelle environment and delays the onset of unfolding. Hence, it is likely that W42 has a destabilizing effect on the refolded protein. Furthermore, in the case of Ail, once folded, the barrel is likely to retain bound LDAO molecules, which gives rise to the difference in C_m values for anisotropy and f_U calculations. Hysteresis thereby ensues in Ail (discussed later), and W149 may contribute to this process. We do not, however, rule out the possibility that our observations on role of indoles may differ in lipid

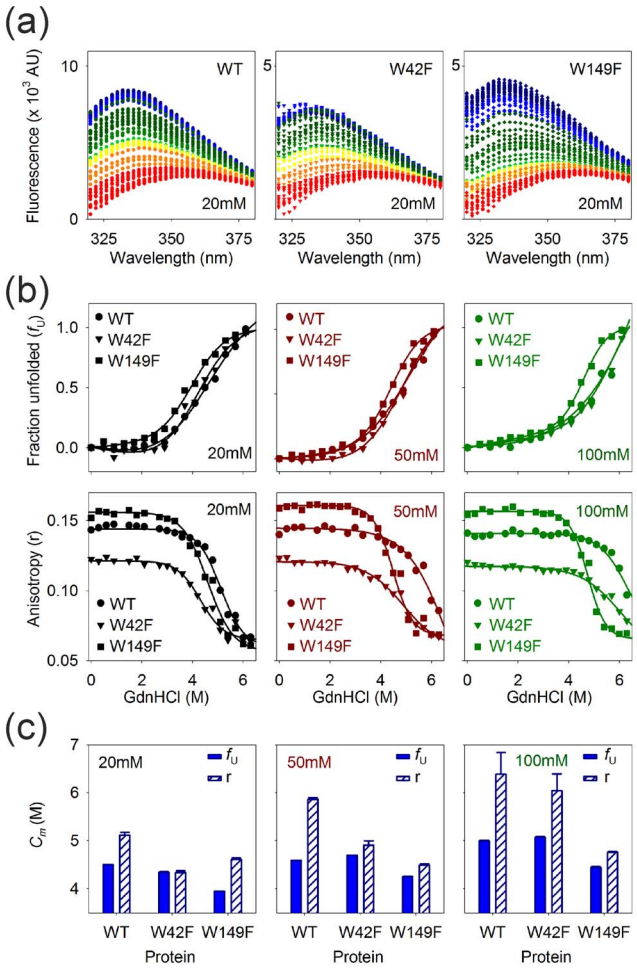

Figure 4 | Ail unfolds in a DPR-dependent manner. (a) Representative Trp emission profiles of Ail-WT and Trp mutants in 20 mM LDAO, highlighting the observed reduction in fluorescence intensity accompanied by a prominent red shift in the $\lambda_{em\text{-}max}$ (depicted in red to blue color scheme), as the refolded protein unfolds when GdnHCl is increased from 0 M to 6.4 M (blue to red). (b) GdnHCl-dependent unfolding of Ail monitored through Trp fluorescence, plotted as the variation in unfolded fractions (f_U) (top graphs), and the corresponding anisotropy (r) change (bottom graphs), with increasing denaturant concentration. Symbol and color codes for Ail-WT (○), W42F (▽) and W149F (□) are black (20 mM), red (50 mM) and green (100 mM) LDAO. Data collected at increments of 0.1 M GdnHCl from two – three independent experiments were used to calculate the mean f_U data set. Shown here are representative points from the mean data without the error bars, for clarity. A representative dataset is provided for anisotropy plots. Fits are shown as solid lines and respective LDAO concentrations are provided in each plot. (c) Plots of C_m values obtained from f_U (blue, solid fill) and anisotropy (r) (blue, diagonal stripes) data for the three Ail constructs across various LDAO concentrations. Note the increase in C_m with increasing LDAO (and DPR) in the case of WT and W42F, while W149F is less affected by changes in DPR. Error bars represent goodness of fits. Also see Supplementary Figs. 5–9.

systems *versus* detergent micelles employed in this study. For instance, earlier studies using other β-barrels have observed substantial variations in barrel (un/re)folding kinetics in lipid vesicles *versus* micelles[16,19,33,49,53,54].

It is tempting to propose that W149 has little role during folding, but establishes stereospecific contacts after barrel formation is completed. Such interactions are critical for subsequent Ail stability and are not mimicked by Phe in that position[39,52]. On the other hand, presence of W42 seems to be necessary only for the refolding process and does not contribute to the subsequent stability of the folded protein. Comparable data for the WT and W149F (Fig. 2 and Fig. 3) and several instances of similar behaviour of refolded WT and W42F Ail (see Fig. 4b f_U C_m) support the importance of W42 during barrel formation and W149 for barrel stabilization (Fig. 6). Such positional contribution of indoles could evolutionarily demarcate various 8-stranded β-barrels. For instance, the close homologue of *Yersinia* Ail in *E. coli*, namely, OmpX, shows unusual thermal stability and is resistant to aggregation in LDAO micelles[42]. Despite > 40% identity in sequence and nearly superposable structures[25], the distribution of aromatics, particularly the positioning of W42 (of Ail) *versus* W76 (of OmpX), is different in both proteins. Likewise, a thermodynamic study on Trp mutants of another 8-stranded TM barrel from *E. coli*, outer membrane protein A, shows a global reduction in barrel stability upon mutation of several Trp residues[32,33,38,55]. Put together, this suggests that a contextual evaluation of aromatic contributions to β-barrels is necessary[30–33,39,52].

The elaborate assembly of transmembrane β-barrels necessitates that the folding equilibrium is sizably favoured towards a stable refolded protein. Such complex folding pathways oftentimes result in kinetically trapped proteins that display hysteresis and/or irreversibility in their barrel formation pathway. While thermodynamic equilibrium can be achieved for similar 8-stranded TM β-barrels such as OmpA and PagP[14,15,19,32,33], other studies have recognized the different responses elicited by the folding and unfolding kinetics of these barrels to factors such as lipid concentrations[14,18,36,56]. Residue-wise contributions, based on stereospecific positioning, and protein-lipid interaction mechanisms[31,32,57,58], may together heavily impact (un)folding rates and pathways, giving rise to the observed hysteresis. Such kinetic stability may be critical, for outer membrane protein function in hostile environments, and mandated by the low protein recycling observed for TM barrels.

In LDAO micelles, the Ail protein of pathogenic *Yersinia* is kinetically stabilized, which we deduce from the observed hysteresis in the folding/unfolding pathways, and the differential responses of both mechanisms to the presence of chemical denaturants (Fig. 5). Such hysteresis in Ail is likely to arise from differences in the activation energy barrier for the folding/unfolding events, giving rise to different apparent free energy values (Supplementary Table 1). In GdnHCl, while we obtain reversibility, hysteresis may be introduced in either the refolding or the unfolding process[15]. Indeed, a comparison of the C_m values (Supplementary Fig. 13a, bottom panel) of both processes derived from f_U plots (Supplementary Fig. 13a, top panel), clearly demarcates the DPR dependence of the *unfolding* process, suggesting that in Ail, this event falls outside experimentally quantifiable timescales. While considerable unfolding can still be achieved in Ail in ~24 h, studies on OmpA have demonstrated this process to be sizeably slow, attaining completion in days (GdnHCl-denatured) to weeks (urea-denatured), or may require higher temperatures[16,19,54]. A similar pattern from the anisotropy C_m supports our conclusions that the presence of excess LDAO (up to 100 mM) stabilizes the refolded protein and slows the onset of unfolding. Moreover, we can achieve Ail refolding within minutes, under ambient conditions, indicating that barrel formation is spontaneous when denaturant levels are sufficiently lowered.

By and large, the prolonged unfolding timescales of Ail barrel in high DPR is akin to the slow unfolding of green fluorescent protein, wherein chromophore formation by the covalent modification, leads to a 'dual-basin' energy landscape in equilibrium (un)folding experiments of this protein[59]. In Ail, such 'locked' barrel structures are facilitated by stabilizing interactions of the transmembrane segment with its surrounding lipid or detergent environment. These interactions are directed by the transmembrane W149, which contributes significantly to the high $\Delta G^{0,F}_{app}$ even in micellar systems (see Supplementary Table 1), and dictate barrel stability against both

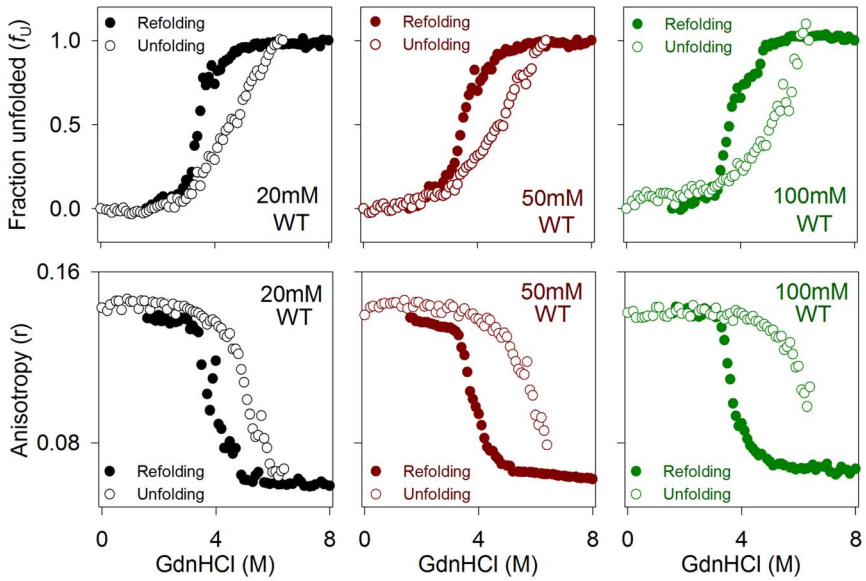

Figure 5 | Hysteresis in Ail arises from variations in barrel-micelle interaction efficacy. (Top) Comparison of the GdnHCl-mediated refolding (filled circles) and unfolding (open circles) curves, shown here for Ail-WT. Data were obtained from unfolded fractions (f_U) derived from Trp fluorescence, in 20 mM (black), 50 mM (red) and 100 mM (green) LDAO. The mean values from independent experiments are provided here, without error bars. Notice the cooperativity of the refolding reaction, and the comparatively low cooperativity of the unfolding reaction. (Bottom) Representative Trp anisotropy values obtained for the GdnHCl-mediated refolding (filled circles) and unfolding (open circles) of WT Ail. Note that while the f_U data for the unfolding experiment tends to 1.0 in 100 mM LDAO (top panel), the corresponding anisotropy values do not reach ~0.06 (for a fully unfolded protein), suggesting that unfolded Ail probably binds substantially to LDAO in the vicinity of the aromatics. A similar color scheme is retained in all datasets. Also see Supplementary Fig. 13.

chemical (Fig. 6) and thermal denaturants (not shown). While the probe position may influence our conclusions, parameters derived for the WT *versus* Trp mutants are not additive, suggesting that the Trp residue contribution to Ail behaviour is substantial, and masks positional contributions of the fluorophore to the data.

Owing to its amphipathic nature, the indole is largely observed at the solvent-lipid interface of membrane proteins, and serves as a stabilizing anchor for the refolded TM domain onto the surrounding lipid membrane, and possesses favourable partition energy between the polar solvent exterior and hydrophobic lipid interior[33]. A recent

Table 2 | Position and distribution of Trp residues in structures of known transmembrane barrels

S. No.[a,b]	PDB ID[c]	Protein[a,b]	# of β-strands[d,e]	# of Trp residues	Position of Trp residue[d]		
					Membrane interface	Transmembrane	Extra-membrane
1	1P4T	NspA	10 (8)	0	-	-	-
2	2POR	Porin	22 (16)	1	1	-	-
3	3QRA	Ail	9 (8)	2	1	1	-
4	1QJ8	OmpX	8 (8)	2	1	1	-
5	2LHF	OprH	10 (8)	2	2	-	-
6	3HW9	OmpF	25 (16)	2	1	1	-
7	1E54	Omp32	24 (16)	2	-	1	1
8	3DZM	TtoA	14 (8)	3	1	-	2
9	3FID	LpxR	17 (12)	3	-	1	2
10	2X27	OprG	17 (8)	4	4	-	-
11	3BRY	TbuX	27 (14)	4	2	2	-
12	1K24	OpcA	15 (10)	4	3	1	-
13	1UYN	NalP	14 (12)	4	3	-	1
14	1H6S	Porin	19 (16)	4	3	1	-
15	3EMO	Hia	[6 (4)]x3[f]	1	1	-	-
16	4FQE	KdgM	14 (12)	3	2	-	1
17	1UUN	MspA	[14 (2)]x8[f]	4	3	1	-
18	3WI4	PorB	[22 (16)]x3[f]	4	3	-	1
19	1WP1	OprM	[13 (4)]x3[f]	4	2	-	2
20	2LME	YadA	[5 (4)]x3[f]	2	1	-	1

[a]Non-redundant structures were retrieved from PDBTM: Protein Data Bank of Transmembrane Proteins; http://pdbtm.enzim.hu/. Only proteins with a maximum of four Trp residues are listed.
[b]Examples 15-19 have been classified as porins in PDB; 20 is an anchor protein.
[c]PDB: RCSB Protein Data Bank; http://www.rcsb.org/pdb.
[d]Information derived from both PDBTM and PDB.
[e]Numbers provided represent the total number of β-strands in the structure and those in brackets represent the total number of transmembrane β-strands.
[f][Number of strands in one monomer (Number of transmembrane strands in one monomer)] x Number of monomers.

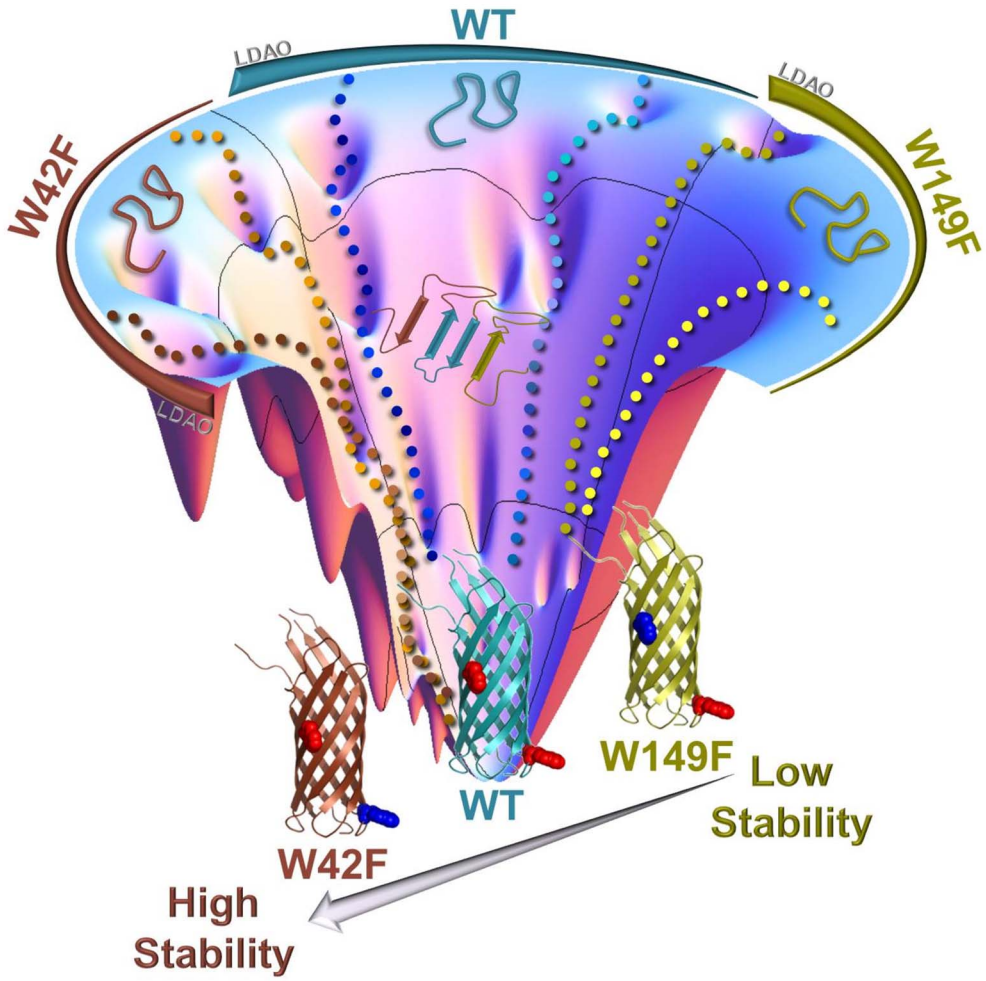

Figure 6 | Schematic highlighting the contribution of W42 and W149 in the folding and stability of Ail in LDAO micelles. WT Ail (blue/cyan) is shown in the center, W42F (brown) is shown to the left and W149F (green/yellow) to the right of the folding funnel. Dotted lines depict possible folding pathways on the folding funnel (generated using a Mathematica® notebook available at www.oaslab.com). W42 of Ail plays a key role in driving barrel refolding and therefore mutation of this residue populates refolding intermediates during barrel formation, as depicted here for the W42F mutant (brown). Furthermore, presence of only W42 (in the W149F mutant) lowers the incidence of stable intermediates in the refolding pathway. In all three proteins, increasing the LDAO concentration affects the folding efficiency by stabilizing the on-pathway intermediates. Once folded, barrel stability is determined by W149, and the three proteins now follow the order W42F > WT > W149F. The most favorable free energy minimum in LDAO micelles is achieved in the Ail barrel possessing a single W149 in the transmembrane region.

study that estimated the influence of lipid solvation of Trp residues of *E. coli* OmpA found greater β-barrel stabilization when the indole is buried, i.e., is highly lipid solvated (buried indole)[36]. A complementary report investigating multi-pass TM helices provides contrasting evidence, wherein preferential interfacial Trp localization and a noticeable affinity of Phe for the lipid core were obtained[52]. Another elaborate study on the Trp residues of *E. coli* OmpA (outer membrane protein A) has identified a contribution of -2.0 kcal/mol and -1.0 kcal/mol for isolated interfacial Trp and Phe, respectively[32,33]. Our study re-affirms the concurrent existence of both indole preferences, which stems from the differential functions of both Ail indoles. W42 possesses characteristics of a rigid indole that is favourably localized at the solvent-micelle interface, while W149 is a dynamic micelle-embedded tryptophan. This disparity in indole contribution influences barrel stability in various DPRs, serving as the major deciding element for hysteresis in Ail.

It has not escaped our notice that the W42F mutant, in addition to retaining W149, also has a F42, which may together contribute to the high (kinetic) stability (Fig. 6)[39]. However, a Trp-less Ail displays only marginally superior barrel stability over the W149F mutant (data not shown), indicating that it is indeed W149 that is necessary for the observed characteristics of the Ail barrel. It is therefore intriguing why a single Trp mutant was not evolutionarily selected over the WT Ail with two tryptophans. Analysis of Trp distribution across known TM β-barrels (72 non-redundant structures) reveals only two proteins having fewer than two Trp residues (Table 2). Mapping the location of Trp residues in those proteins (with upto 4 Trp residues are listed in Table 2), clearly indicates that the indole is preferentially located at the interface. Further, mutational studies on PagP have shown that extra-membrane interface indoles are also important for barrel stability[60]. Our data also points to the necessity of W42 to assist protein folding, while W149 warrants subsequent β-barrel stability. We conjecture that Ail, and possibly other homologous barrels, have evolutionarily attained a balance between the folding and unfolding events by favouring Trp residues (in place of Phe) at the solvent-lipid interface. It would be interesting to address whether the indole ring has additional roles or is merely an evolutionary accident.

Our current study provides a unique insight on the selective contributions of W42 to Ail folding and W149 to kinetic stability of the refolded Ail β-barrel (and the associated hysteresis). This is the first

report, to our knowledge, of differential Trp contributions to the refolding pathway and unfolding event of a β-barrel membrane protein, as well as increased barrel stability upon mutation of a tryptophan (in Ail-W42F). Our study contradicts the several reports that attribute TM α-helical or β-barrel stability to the presence of interface Trp residues in the sequence[31–37,39,57,61]. At this juncture, one may expect that kinetic stability modulated by the surrounding lipid amounts provides the necessary malleability to steer efficient Ail functioning in Yop delivery during *Yersinia* infection. Indeed Ail behaviour is vastly different from the thermodynamic properties of its close homologue OmpX. Detailed analysis of such biophysical characteristics of Ail will also expedite the development of structure-based drugs and vaccines against plague.

Methods

Protein preparation. Gene corresponding to the mature Ail protein (without the signal sequence) was cloned in pET-3b vector, expressed as inclusion bodies in *E. coli* C41 cells[24], and purified on a cation exchange column, using minor modifications of reported protocols[24,42]. Single Trp mutants (W42F and W149F) were generated using site directed mutagenesis, and purified using similar methods. The mutation was characterized by DNA sequencing of the genes and mass spectrometric fingerprinting of the expressed proteins (not shown). Refolding was achieved by rapid 10-fold dilution of 25 μg/μL Ail from 8.0 M GdnHCl, into the refolding reaction, consisting of 100 mM, 250 mM or 500 mM LDAO prepared in 20 mM Tris-HCl pH 8.5, at 25°C. Protein quantitation was achieved by A_{280}, using an extinction coefficient of 28880 M^{-1} cm^{-1} and 23380 M^{-1} cm^{-1} for WT and Trp mutants, respectively.

Refolded samples were dialyzed to remove excessive GdnHCl, followed by extensive centrifugation, to obtain the 5X refolding stocks. These stocks contained 2.5 μg/μL Ail (~140 μM) and 100 mM, 250 mM or 500 mM LDAO in 20 mM Tris-HCl pH 8.5 and trace amounts of GdnHCl. The final DPRs achieved in chemical and thermal denaturation experiments were ~700 : 1 (for 20 mM LDAO), ~1750 : 1 (for 50 mM LDAO) and ~3500 : 1 (for 100 mM LDAO), in 20 mM Tris-HCl pH 8.5, unless stated otherwise. At these LDAO concentrations, micellar forms of the detergent were persistent even in high denaturant concentrations(Supplementary Figs. 10–12), and thereby did not give rise to artefacts in our unfolding experiments due to the dissolution of LDAO micelles by high GdnHCl employed in our equilibrium (un/re)folding experiments.

Gel quantification and proteolysis. Quantification of the refolding reaction was achieved by densitometry, as described earlier[42]. Proteolysis was carried out as reported earlier[42], with minor modifications. Briefly, proteinase K was added to the refolding reaction to a final concentration of 2.0 μg/μl and incubated at 25°C for ~15 min, prior to loading on the gel. At these proteinase K concentrations, we could not completely arrest the protease activity using frequently used inhibitors. Reactions were therefore diluted to a final LDAO concentration of ≤20 mM using gel loading dye (as high LDAO interferes with band migration), and analyzed on 15% SDS-PAGE.

Fluorescence measurements. Trp fluorescence emission spectra, acrylamide quenching (without inner filter correction) and calculation of the Stern-Volmer constant (K_{SV}), as well as measurement of average lifetimes ($<\tau>$) were carried out in various DPRs for the refolded proteins and denatured controls, using reported protocols[18,62]. Bimolecular quenching constant (k_q) was derived using the formula $k_q = K_{SV}/<\tau>$[45].

Equilibrium unfolding and refolding. (Un/re)folding experiments were carried out as described earlier[44]. Briefly, (un)folded 5X protein stocks in LDAO with or without 8.0 M GdnHCl, respectively, were diluted into a GdnHCl gradient, while the protein and LDAO concentrations were maintained at 0.5 μg/μl (~28 μM) and 20, 50 or 100 mM, respectively. Progress of all reactions was monitored for 48 h, using Trp fluorescence between 320–380 nm, using a $\lambda_{ex\text{-}max}$ = 295 nm. Equilibrium was achieved in ~24 h (Supplementary Fig. 14) and no further change in the fluorescence intensity was observed upon prolonged incubation. Based on comparison of the fluorescence intensities observed for the unfolded protein prepared under identical sample/buffer conditions, it was estimated that ~95% of refolded Ail could be successfully unfolded by ~24 h in 6.4 M GdnHCl (see Supplementary Figs. 5–7). Since no further significant change in the sample fluorescence was observed, the apparent free energy values were derived for the 48 h data (described below). Anisotropy (r) values were recorded at the end-points (48 h).

For fluorescence measurements, plots of (un)folded fractions (f_U or f_F) *versus* GdnHCl were generated using the observed intensity at 330 nm, as described[15,63], and analyzed by linear extrapolation[19,36,44,63], to derive the mid-point(s) of chemical (de/re)naturation (C_m), $\Delta G^{0,F}_{app}$ and $\Delta G^{0,U}_{app}$ (apparent folding and unfolding free energy at 48 h) and m_{app} (apparent (un)folding cooperativity at 48 h). In refolding experiments that showed an intermediate species, transition from the intermediate to the folded form was used to derive all the thermodynamic parameters by linear extrapolation. Anisotropy data were fit to two- or three-state equations[17,63], and only C_m values were considered.

1. Kleinschmidt, J. H. & Tamm, L. K. Folding intermediates of a beta-barrel membrane protein. Kinetic evidence for a multi-step membrane insertion mechanism. *Biochemistry* **35**, 12993–13000 (1996).
2. Jayaraman, S., Gantz, D. L. & Gursky, O. Kinetic stabilization and fusion of apolipoprotein A-2:DMPC disks: comparison with apoA-1 and apoC-1. *Biophys. J.* **88**, 2907–2918 (2005).
3. Curnow, P. & Booth, P. J. Combined kinetic and thermodynamic analysis of alpha-helical membrane protein unfolding. *Proc. Natl. Acad. Sci. U. S. A.* **104**, 18970–18975 (2007).
4. Jefferson, R. E., Blois, T. M. & Bowie, J. U. Membrane proteins can have high kinetic stability. *J. Am. Chem. Soc.* **135**, 15183–15190 (2013).
5. Popot, J. L. & Engelman, D. M. Membrane protein folding and oligomerization: the two-stage model. *Biochemistry* **29**, 4031–4037 (1990).
6. Sanchez-Ruiz, J. M. Theoretical analysis of Lumry-Eyring models in differential scanning calorimetry. *Biophys. J.* **61**, 921–935 (1992).
7. Haltia, T. & Freire, E. Forces and factors that contribute to the structural stability of membrane proteins. *Biochim. Biophys. Acta* **1228**, 1–27 (1995).
8. Engelman, D. M. *et al.* Membrane protein folding: beyond the two stage model. *FEBS Lett.* **555**, 122–125 (2003).
9. Sanchez-Ruiz, J. M. Protein kinetic stability. *Biophys. Chem.* **148**, 1–15 (2010).
10. Moon, C. P., Kwon, S. & Fleming, K. G. Overcoming hysteresis to attain reversible equilibrium folding for outer membrane phospholipase A in phospholipid bilayers. *J. Mol. Biol.* **413**, 484–494 (2011).
11. Andrews, B. T., Capraro, D. T., Sulkowska, J. I., Onuchic, J. N. & Jennings, P. A. Hysteresis as a Marker for Complex, Overlapping Landscapes in Proteins. *J. Phys. Chem. Lett.* **4**, 180–188 (2013).
12. Otzen, D. E. & Andersen, K. K. Folding of outer membrane proteins. *Arch. Biochem. Biophys.* **531**, 34–43 (2013).
13. Booth, P. J. & Curnow, P. Folding scene investigation: membrane proteins. *Curr. Opin. Struct. Biol.* **19**, 8–13 (2009).
14. Huysmans, G. H., Baldwin, S. A., Brockwell, D. J. & Radford, S. E. The transition state for folding of an outer membrane protein. *Proc. Natl. Acad. Sci. U. S. A.* **107**, 4099–4104 (2010).
15. Moon, C. P., Zaccai, N. R., Fleming, P. J., Gessmann, D. & Fleming, K. G. Membrane protein thermodynamic stability may serve as the energy sink for sorting in the periplasm. *Proc. Natl. Acad. Sci. U. S. A.* **110**, 4285–4290 (2013).
16. Hong, H. & Tamm, L. K. Elastic coupling of integral membrane protein stability to lipid bilayer forces. *Proc. Natl. Acad. Sci. U. S. A.* **101**, 4065–4070 (2004).
17. Moon, C. P. & Fleming, K. G. Side-chain hydrophobicity scale derived from transmembrane protein folding into lipid bilayers. *Proc. Natl. Acad. Sci. U. S. A.* **108**, 10174–10177 (2011).
18. Maurya, S. R. & Mahalakshmi, R. Modulation of Human Mitochondrial Voltage-Dependent Anion Channel 2 (hVDAC-2) Structural Stability by Cysteine-Assisted Barrel-Lipid Interactions. *J. Biol. Chem.* **288**, 25584–25592 (2013).
19. Andersen, K. K., Wang, H. & Otzen, D. E. A kinetic analysis of the folding and unfolding of OmpA in urea and guanidinium chloride: single and parallel pathways. *Biochemistry* **51**, 8371–8383 (2012).
20. Maurya, S. R. & Mahalakshmi, R. Influence of Protein - Micelle Ratios and Cysteine Residues on the Kinetic Stability and Unfolding Rates of Human Mitochondrial VDAC-2. *PLoS One* **9**, e87701 (2014).
21. Stanley, A. M. & Fleming, K. G. The process of folding proteins into membranes: challenges and progress. *Arch. Biochem. Biophys.* **469**, 46–66 (2008).
22. Otzen, D. E. Protein unfolding in detergents: effect of micelle structure, ionic strength, pH, and temperature. *Biophys. J.* **83**, 2219–2230 (2002).
23. Kolodziejek, A. M. *et al.* Phenotypic characterization of OmpX, an Ail homologue of Yersinia pestis KIM. *Microbiology* **153**, 2941–2951 (2007).
24. Plesniak, L. A. *et al.* Expression, refolding, and initial structural characterization of the Y. pestis Ail outer membrane protein in lipids. *Biochim. Biophys. Acta* **1808**, 482–489 (2011).
25. Yamashita, S. *et al.* Structural insights into Ail-mediated adhesion in Yersinia pestis. *Structure* **19**, 1672–1682 (2011).
26. Kolodziejek, A. M., Hovde, C. J. & Minnich, S. A. Yersinia pestis Ail: multiple roles of a single protein. *Front. Cell Infect. Microbiol.* **2**, 103 (2012).
27. Bliska, J. B. & Falkow, S. Bacterial resistance to complement killing mediated by the Ail protein of Yersinia enterocolitica. *Proc. Natl. Acad. Sci. U. S. A.* **89**, 3561–3565 (1992).
28. Felek, S. & Krukonis, E. S. The Yersinia pestis Ail protein mediates binding and Yop delivery to host cells required for plague virulence. *Infect. Immun.* **77**, 825–836 (2009).
29. Killian, J. A. *et al.* Modulation of membrane structure and function by hydrophobic mismatch between proteins and lipids. *Pure Appl. Chem.* **70**, 75–82 (1998).
30. Yau, W. M., Wimley, W. C., Gawrisch, K. & White, S. H. The preference of tryptophan for membrane interfaces. *Biochemistry* **37**, 14713–14718 (1998).
31. Killian, J. A. & von Heijne, G. How proteins adapt to a membrane-water interface. *Trends Biochem. Sci.* **25**, 429–434 (2000).
32. Hong, H., Park, S., Jimenez, R. H., Rinehart, D. & Tamm, L. K. Role of aromatic side chains in the folding and thermodynamic stability of integral membrane proteins. *J. Am. Chem. Soc.* **129**, 8320–8327 (2007).
33. Sanchez, K. M., Gable, J. E., Schlamadinger, D. E. & Kim, J. E. Effects of tryptophan microenvironment, soluble domain, and vesicle size on the thermodynamics of

membrane protein folding: lessons from the transmembrane protein OmpA. *Biochemistry* **47**, 12844–12852 (2008).
34. Sun. H., Greathouse. D. V., Andersen. O. S. & Koeppe. R. E. 2nd. The preference of tryptophan for membrane interfaces: insights from N-methylation of tryptophans in gramicidin channels. *J. Biol. Chem.* **283**, 22233–22243 (2008).
35. de Jesus, A. J. & Allen, T. W. The role of tryptophan side chains in membrane protein anchoring and hydrophobic mismatch. *Biochim. Biophys. Acta* **1828**, 864–876 (2013).
36. Hong, H., Rinehart, D. & Tamm, L. K. Membrane depth-dependent energetic contribution of the tryptophan side chain to the stability of integral membrane proteins. *Biochemistry* **52**, 4413–4421 (2013).
37. Lasalde, J. A. *et al*. Tryptophan substitutions at the lipid-exposed transmembrane segment M4 of Torpedo californica acetylcholine receptor govern channel gating. *Biochemistry* **35**, 14139–14148 (1996).
38. Kleinschmidt, J. H., den Blaauwen, T., Driessen, A. J. & Tamm, L. K. Outer membrane protein A of Escherichia coli inserts and folds into lipid bilayers by a concerted mechanism. *Biochemistry* **38**, 5006–5016 (1999).
39. Bielecki, M., Wojtowicz, H. & Olczak, T. Differential roles of tryptophan residues in conformational stability of Porphyromonas gingivalis HmuY hemophore. *BMC Biochem.* **15**, 2 (2014).
40. Burgess, N. K., Dao, T. P., Stanley, A. M. & Fleming, K. G. Beta-barrel proteins that reside in the Escherichia coli outer membrane in vivo demonstrate varied folding behavior in vitro. *J. Biol. Chem.* **283**, 26748–26758 (2008).
41. Mahalakshmi, R. & Marassi, F. M. Orientation of the Escherichia coli outer membrane protein OmpX in phospholipid bilayer membranes determined by solid-State NMR. *Biochemistry* **47**, 6531–6538 (2008).
42. Maurya, S. R., Chaturvedi, D. & Mahalakshmi, R. Modulating lipid dynamics and membrane fluidity to drive rapid folding of a transmembrane barrel. *Sci. Rep.* **3**, 1989 (2013).
43. Wang, H., Andersen, K. K., Vad, B. S. & Otzen, D. E. OmpA can form folded and unfolded oligomers. *Biochim. Biophys. Acta* **1834**, 127–136 (2013).
44. Chaturvedi, D. & Mahalakshmi, R. Methionine Mutations of Outer Membrane Protein X Influence Structural Stability and beta-Barrel Unfolding. *PLoS One* **8**, e79351 (2013).
45. Lakowicz, J. R. *Principles of Fluorescence Spectroscopy*. (Springer London, Limited, 2009).
46. Zurawa-Janicka, D. *et al*. Temperature-induced changes of HtrA2(Omi) protease activity and structure. *Cell Stress Chaperon.* **18**, 35–51 (2013).
47. Kaufmann, T. C. *Detergent-protein and Detergent-lipid Interactions: Implications for Two-dimensional Crystallization of Membrane Proteins and Development of Tools for High Throughput Crystallography* Doctor of Philosophy thesis, University of Basel, (2006).
48. Kleinschmidt, J. H., Wiener, M. C. & Tamm, L. K. Outer membrane protein A of E. coli folds into detergent micelles, but not in the presence of monomeric detergent. *Protein Sci.* **8**, 2065–2071 (1999).
49. Pocanschi, C. L. *et al*. The major outer membrane protein of Fusobacterium nucleatum (FomA) folds and inserts into lipid bilayers via parallel folding pathways. *J. Mol. Biol.* **355**, 548–561 (2006).
50. Shanmugavadivu, B., Apell, H. J., Meins, T., Zeth, K. & Kleinschmidt, J. H. Correct folding of the beta-barrel of the human membrane protein VDAC requires a lipid bilayer. *J. Mol. Biol.* **368**, 66–78 (2007).
51. Anbazhagan, V., Vijay, N., Kleinschmidt, J. H. & Marsh, D. Protein-lipid interactions with Fusobacterium nucleatum major outer membrane protein FomA: spin-label EPR and polarized infrared spectroscopy. *Biochemistry* **47**, 8414–8423 (2008).
52. Braun, P. & von Heijne, G. The aromatic residues Trp and Phe have different effects on the positioning of a transmembrane helix in the microsomal membrane. *Biochemistry* **38**, 9778–9782 (1999).
53. Pocanschi, C. L., Patel, G. J., Marsh, D. & Kleinschmidt, J. H. Curvature elasticity and refolding of OmpA in large unilamellar vesicles. *Biophys. J.* **91**, L75–77 (2006).
54. Pocanschi, C. L., Popot, J. L. & Kleinschmidt, J. H. Folding and stability of outer membrane protein A (OmpA) from Escherichia coli in an amphipathic polymer, amphipol A8-35. *Eur. Biophys. J.* **42**, 103–118 (2013).
55. Sanchez, K. M., Kang, G., Wu, B. & Kim, J. E. Tryptophan-lipid interactions in membrane protein folding probed by ultraviolet resonance Raman and fluorescence spectroscopy. *Biophys. J.* **100**, 2121–2130 (2011).
56. Kleinschmidt, J. H. & Tamm, L. K. Secondary and tertiary structure formation of the beta-barrel membrane protein OmpA is synchronized and depends on membrane thickness. *J. Mol. Biol.* **324**, 319–330 (2002).
57. Rasmussen, A. *et al*. The role of tryptophan residues in the function and stability of the mechanosensitive channel MscS from Escherichia coli. *Biochemistry* **46**, 10899–10908 (2007).
58. Sanders, C. R. & Mittendorf, K. F. Tolerance to changes in membrane lipid composition as a selected trait of membrane proteins. *Biochemistry* **50**, 7858–7867 (2011).
59. Andrews, B. T., Gosavi, S., Finke, J. M., Onuchic, J. N. & Jennings, P. A. The dual-basin landscape in GFP folding. *Proc. Natl. Acad. Sci. U. S. A.* **105**, 12283–12288 (2008).
60. Huysmans, G. H., Radford, S. E., Brockwell, D. J. & Baldwin, S. A. The N-terminal helix is a post-assembly clamp in the bacterial outer membrane protein PagP. *J. Mol. Biol.* **373**, 529–540 (2007).
61. Markovic-Housley, Z., Stolz, B., Lanz, R. & Erni, B. Effects of tryptophan to phenylalanine substitutions on the structure, stability, and enzyme activity of the IIAB(Man) subunit of the mannose transporter of Escherichia coli. *Protein Sci.* **8**, 1530–1535 (1999).
62. Maurya, S. R. & Mahalakshmi, R. Cysteine residues impact the stability and micelle interaction dynamics of the human mitochondrial beta-barrel anion channel hVDAC-2. *PLoS One* **9**, e92183 (2014).
63. Moon, C. P. & Fleming, K. G. Using tryptophan fluorescence to measure the stability of membrane proteins folded in liposomes. *Methods Enzymol.* **492**, 189–211 (2011).

Acknowledgments

The authors thank T. Madhumohan for initial optimization of Ail refolding. A.G. acknowledges research fellowship from IISER Bhopal. R.M. is a recipient of the Ramalingaswami Fellowship from the Department of Biotechnology, Government of India. This work is supported by the Science Engineering and Research Board of the Department of Science and Technology grant SR/FT/LS-47/2010 and Department of Biotechnology grant BT/HRD/35/02/25/2009, from the Government of India to R.M.

Author contributions

R.M. conceived the study and designed the overall strategy; A.G. and P.Z. carried out the experiments. R.M. wrote the manuscript with significant input from A.G. and P.Z.

Additional information

Supplementary information accompanies this paper at http://www.nature.com/scientificreports

Competing financial interests: The authors declare no competing financial interests.

How to cite this article: Gupta, A., Zadafiya, P. & Mahalakshmi, R. Differential Contribution of Tryptophans to the Folding and Stability of the Attachment Invasion Locus Transmembrane β-Barrel from *Yersinia pestis*. *Sci. Rep.* **4**, 6508; DOI:10.1038/srep06508 (2014).